

Localized indentation of sandwich beam with metallic foam core

Zhongyou Xie^{1,2}, Zhijun Zheng¹ and Jilin Yu¹

Abstract

The localized behavior of sandwich structures with foam core subjected to indentation loading is investigated in this article. Based on the principle of virtual velocities, concisely explicit solutions for the indentation forces and shape functions of deformation zones of sandwich beams are derived. Both flat and cylindrical indenters are considered. The indentation force varies linearly with the square root of indenter displacement and the surface deformation profiles are proportional to the square of the distance from the contact center along the beam direction. Finite element models have been established using the ABAQUS/Explicit code to verify the validity and applicability of the analytical solutions. The theoretical predictions of the profiles of deformation zones and the denting loads of indenters are in good agreement with those by numerical simulation.

Keywords

foam core, localized indentation, principle of virtual velocities, sandwich beam

Introduction

Composite sandwich structures subjected to local loading such as bird strikes, runway debris, and tool drops during maintenance are prone to damage due to their low bending resistance of thin faces and low strength of core material. A residual dent significantly degrades the mechanical properties of the sandwich structures, and there is an evident need for a concise and reliable analytical method for predicting their response to local loading.

¹CAS Key Laboratory of Mechanical Behavior and Design of Materials, University of Science and Technology of China, Hefei, Anhui 230026, PR China

²Department of Civil and Architectural Engineering, Tongling University, Tongling, Anhui 244000, PR China

Corresponding author:

Zhijun Zheng, CAS Key Laboratory of Mechanical Behavior and Design of Materials, University of Science and Technology of China, Hefei, Anhui 230026, PR China

Email: zjzheng@ustc.edu.cn

The response of foam-core sandwich structures to indentation has been studied extensively in the last decade. Besides many experimental investigations and numerical simulations, some analytical models were established. Gdoutos et al. [1] studied the indentation of a sandwich panel experimentally and the problem was modeled as an elastic beam resting on a Winkler elastic-plastic foundation. Soden [2] modeled the core as a rigid-perfectly plastic foundation, which led to a simple expression for the failure load of facing fracture for the indentation of composite sandwich beams. Shuaieb and Soden [3] predicted indentation failure loads for sandwich beams with foam cores, which were modeled as an elastic beam resting on an elastic-plastic foundation. Zenkert et al. [4] further considered the unloading response, including the residual dent and the residual strain levels in the core. Koissin et al. [5, 6] studied the inelastic response of sandwich structures to local loading using the Kirchhoff-Love theory for the skin while the core was assumed to be elastic-perfectly plastic. More recently, Koissin and Shipsha [7] investigated the residual denting of the face sheet and corresponding core damage, which was analytically considered in the context of elastic bending of the face sheet accompanied by nonlinear deformation of the crushed foam core. Minakuchi et al. [8] established a 'segment-wise model' for indentation loading and unloading responses of honeycomb sandwich beams, where the beam was divided into many segments based on the periodic structure and the core behavior was approximately described by a set of lines according to the testing results.

In all these models the face sheet was assumed to be elastic, which is true for face sheets made of fiber-reinforced composites. However, when sandwiched structures with metal skins and metallic foam core are considered, the face sheet will deform plastically, so it is of great importance to obtain solutions of plastic response under a larger deflection.

The indentation responses of foam sandwich structure loaded by a finite indenter were analyzed in this study. The variation of size of indentation dents was analyzed in terms of the analytical results. To verify the validity and applicability of the analytical solutions, an FEA model was established using the ABAQUS code.

Localized indentation models

The deformation of a sandwich beam with metallic foam loaded by an indenter is usually complex. Here, we focus on the localized indentation without considering the overall bending of the beam. Two types of rigid indenters, i.e., flat and cylindrical indenters, are considered, as schematically represented in Figure 1. The structure with width b has an infinite length and is composed of two face sheets and a foam core with thicknesses h and c , respectively. The flow stress of the face sheet material is σ_0 . The foam core has a constant plateau stress σ_p . The indentation displacement of the indenter is denoted by δ , while that of the outer zone is represented by $w(x)$ with x being the horizontal coordinate. The length of the deformed region is denoted by 2ξ which will be determined later. The width

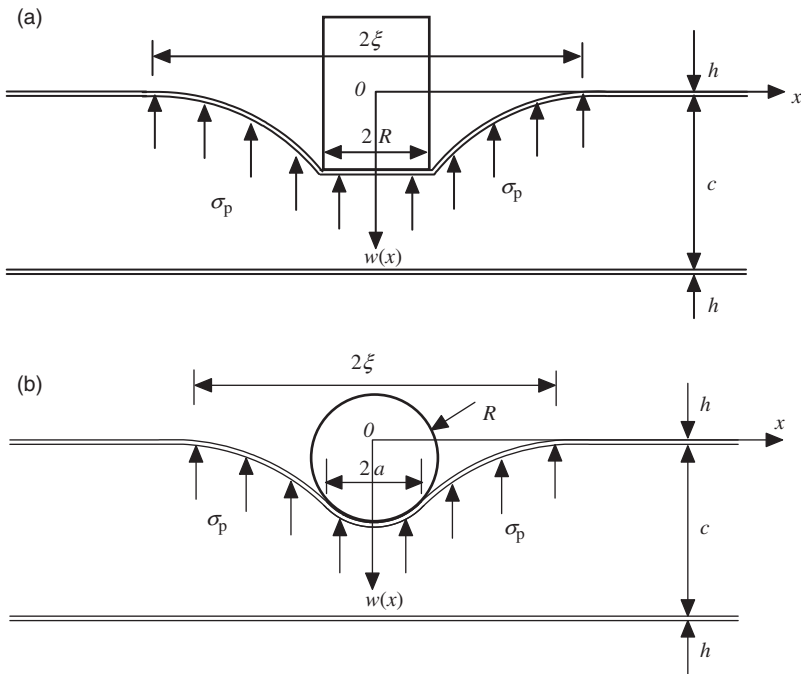


Figure 1. Schematic profile of the deforming zone: (a) under a flat indenter and (b) under a cylindrical indenter.

of the flat indenter is $2R$, as marked in Figure 1(a). The width of the contact region between the cylindrical indenter with radius R and the top face sheet is $2a$, see Figure 1(b).

Elastic response of the composite structure is neglected from the present model. The upper face sheet is modeled as an infinite, ideally plastic thin plate resting on a rigid-plastic foundation, which gives a constant crushing resistance by the foam core. The principle of virtual velocities is employed to investigate the localized indentation behavior of sandwich beam. The statement of energy equilibrium requires that the rate of external work equals to the total rate of internal energy dissipation, i.e.,

$$\dot{W}_{\text{ext}} = \dot{W}_{\text{int}} \tag{1}$$

The rate of work by external force is

$$\dot{W}_{\text{ext}} = P\dot{\delta} \tag{2}$$

where P is the indentation force and $\dot{\delta}$ the virtual velocity of the indenter.

Under a flat indenter loading

For the sandwich beam indented by a flat indenter, a close contact between the indenter and the top face sheet of beam is assumed, so the shape function of the contact region can be written as

$$w(x, t) = \delta, \quad 0 \leq |x| \leq R \quad (3)$$

where t represents the time. The velocity field of the dented zone is assumed as

$$\dot{w}(x, t) = \begin{cases} \dot{\delta}, & 0 \leq |x| \leq R, \\ \dot{\delta} \frac{\xi - |x|}{\xi - R}, & R \leq |x| \leq \xi. \end{cases} \quad (4)$$

Thus, the change in the longitudinal curvature becomes zero, i.e., $\dot{\kappa}_x = -\partial^2 \dot{w} / \partial x^2 = 0$, and the rate of internal energy from flexural deformation can be neglected. The strain rate of the upper face sheet is defined according to the theory of moderately large deflection of beam

$$\dot{\epsilon}_x = \frac{dw}{dx} \frac{d\dot{w}}{dx} \quad (5)$$

For the sandwich beam indented by a flat indenter, the contribution to the rate of internal energy dissipation by membrane force in the dented region can be derived from

$$\dot{W}_1 = \int_A N_0 \dot{\epsilon}_x dA = 2 \int_0^\xi N_0 \dot{\epsilon}_x b dx = \frac{2\sigma_0 b h \delta \dot{\delta}}{\xi - R} \quad (6)$$

where $N_0 = \sigma_0 h$. In calculating the formula above, there is no need to know the expression of $w(x)$ due to the linear assumption of the velocity field out of the dented zone. The contribution to the rate of energy dissipation due to compressive deformation of foam core can be calculated by

$$\dot{W}_2 = \int_V \sigma_p d\dot{V} = 2 \int_0^\xi \sigma_p \dot{w} \cdot b dx = \sigma_p b (\xi + R) \dot{\delta} \quad (7)$$

The rate of internal work of the sandwich structure is mainly given by the sum of contributions due to extensional deformation of face sheet and compressive deformation of foam core. Summarizing results of Equations (6) and (7), the total rate of internal energy dissipation, \dot{W}_{int} , is

$$\dot{W}_{\text{int}} = \dot{W}_1 + \dot{W}_2 = \frac{2\sigma_0 b h \delta \dot{\delta}}{\xi - R} + \sigma_p b (\xi + R) \dot{\delta} \quad (8)$$

Submitting Equations (2) and (8) in Equation (1), we have

$$P\dot{\delta} = \frac{2\sigma_0bh\delta\dot{\delta}}{\xi - R} + \sigma_p b(\xi + R)\dot{\delta} \quad (9)$$

Eliminating $\dot{\delta}$ from the above equation, we can determine the indentation force as

$$P = \frac{2\sigma_0bh\delta}{\xi - R} + \sigma_p b(\xi + R) \quad (10)$$

in which the half length of deformation region ξ is still unknown. Based on the principle of minimum work [2], it is required that the half length of deformation region ξ should satisfy the condition of the minimum force for a given indentation displacement, i.e., $\partial P/\partial \xi = 0$. This leads to a relationship between ξ and δ by the following formula

$$\xi = R + (2\sigma_0h\delta/\sigma_p)^{1/2} \quad (11)$$

Substituting the above expression back into Equation (10), we obtain

$$P = 2\sigma_p Rb + 2b(2\sigma_0\sigma_p h\delta)^{1/2} \quad (12)$$

The indentation force is composed by one constant portion due to the finite size of the flat indenter, and another nonconstant portion varying with the square root of the indentation displacement, δ .

The displacement field of the deformation zone could then be calculated by integrating the velocity field with time. For the symmetry, we only consider the case of $x > 0$. Because the extent of the deformed zone ξ also varies with time t , we have

$$w(x, t(\xi)) = \int_{t(x)}^{t(\xi)} \dot{w}(x, t) dt = \int_{t(x)}^{t(\xi)} \dot{\delta} \frac{\xi - x}{\xi - R} dt \quad (13)$$

where $t(x)$ is the time when ξ reaches x . Using Equation (11), we have

$$d\delta = \frac{\sigma_p}{\sigma_0 h} (\xi - R) d\xi \quad (14)$$

Thus, Equation (13) can be rewritten in an alternative form by changing the integration variable from t to ξ through the intermediate variable δ with $d\delta = \dot{\delta} dt$. We get

$$w(x, t) = \frac{\sigma_p}{\sigma_0 h} \int_x^\xi (\xi - x) d\xi = \frac{\sigma_p}{2\sigma_0 h} (\xi - x)^2 \quad (15)$$

Associating the above expression with Equation (11) and considering the symmetry, the deflection profile out of contact region becomes

$$w(x, t) = \delta \left(\frac{\xi - |x|}{\xi - R} \right)^2, \quad R \leq |x| \leq \xi \quad (16)$$

A quadratic form with respect to x is found for the shape function of the top face sheet out of the contact region.

During the indentation of the indenter, the external work is dissipated by the membrane force of face sheet and the compressive deformation of foam core. Integrating Equations (6) and (7) with respect to time t , we can determine the two portions of internal energy as

$$\begin{cases} W_1 = \int_0^t \dot{W}_1 dt = \int_0^\delta \frac{2\sigma_0 b h \delta}{\xi - R} d\delta = \frac{2b}{3} (2\sigma_0 \sigma_p h \delta^3)^{1/2}, \\ W_2 = \int_0^t \dot{W}_2 dt = \int_0^\delta \sigma_p b (\xi + R) d\delta = \frac{2b}{3} (2\sigma_0 \sigma_p h \delta^3)^{1/2} + 2\sigma_p b R \delta. \end{cases} \quad (17)$$

The ratio of the two portions of internal energy is calculated as

$$\alpha = \frac{W_2}{W_1} = 1 + 3 \left(\frac{\sigma_p R^2}{2\sigma_0 h \delta} \right)^{1/2} \quad (18)$$

which varies with δ and is always greater than one. It means more energy is dissipated by the compressive deformation of foam core than that by the membrane force of face sheet during the indentation. Choosing high strength of foam core may help to protect the face sheet effectively.

Under a cylindrical indenter loading

For the sandwich beam indented by a cylindrical indenter, the shape function of contact region between the cylindrical indenter and the top face sheet is

$$w(x, t) = \delta - \left(R - \sqrt{R^2 - x^2} \right) \approx \delta - \frac{x^2}{2R}, \quad 0 \leq |x| \leq a \quad (19)$$

in which, for simplicity, a parabolic approximation has been applied. The velocity field of the dented zone is assumed as

$$\dot{w}(x, t) = \begin{cases} \dot{\delta}, & 0 \leq |x| \leq a, \\ \dot{\delta} \frac{\xi - |x|}{\xi - a}, & a \leq |x| \leq \xi. \end{cases} \quad (20)$$

Similarly as the deduction in the above section, we can determined the two portions of the rates of energy dissipation as

$$\dot{W}_1 = \frac{2\sigma_0 b h \dot{\delta}}{\xi - a} \left(\delta - \frac{a^2}{2R} \right) \quad (21)$$

and

$$\dot{W}_2 = \sigma_p b (\xi + a) \dot{\delta} \quad (22)$$

Thus, the indentation force for the present case could be obtained as

$$P = \frac{2\sigma_0 b h}{\xi - a} \left(\delta - \frac{a^2}{2R} \right) + \sigma_p b (\xi + a) \quad (23)$$

Using the conditions $\partial P / \partial \xi = 0$ and $\partial P / \partial a = 0$, we get

$$\begin{cases} a = [2\sigma_p R^2 \delta / (\sigma_0 h + \sigma_p R)]^{1/2}, \\ \xi = [2(\sigma_0 h + \sigma_p R) \delta / \sigma_p]^{1/2}. \end{cases} \quad (24)$$

By submitting the above result back into Equation (23), the indentation force is determined as

$$P = 2b [2(\sigma_0 h + \sigma_p R) \sigma_p \delta]^{1/2} \quad (25)$$

And similarly, we can obtain the deflection profile of sandwich beam out of the contact region

$$w(x, t) = \left(\delta - \frac{a^2}{2R} \right) \left(\frac{\xi - |x|}{\xi - a} \right)^2, \quad a \leq |x| \leq \xi \quad (26)$$

and the two portions of internal energy

$$\begin{cases} W_1 = \int_0^\delta \frac{2\sigma_0 b h}{\xi - a} \left(\delta - \frac{a^2}{2R} \right) d\delta = \frac{2\sigma_0 b h}{3} \left(\frac{2\sigma_p \delta^3}{\sigma_0 h + \sigma_p R} \right)^{1/2}, \\ W_2 = \int_0^\delta \sigma_p b (\xi + a) d\delta = \frac{2\sigma_0 b h}{3} \left(1 + \frac{2\sigma_p R}{\sigma_0 h} \right) \left(\frac{2\sigma_p \delta^3}{\sigma_0 h + \sigma_p R} \right)^{1/2}. \end{cases} \quad (27)$$

Thus, we have the ratio of the two portions of internal energy

$$\alpha = \frac{W_2}{W_1} = 1 + \frac{2\sigma_p R}{\sigma_0 h} \quad (28)$$

It is interesting to find that this ratio does not depend on the displacement δ but is also greater than one, no matter what the material and structural parameters are.

Finite element modeling

A finite element analysis using the ABAQUS/Explicit code was carried out to verify the validity of the above theoretical predictions. The sandwich structure was laid on a rigid foundation to avoid the overall bending. A one quarter numerical model was established due to symmetry. The indenter was modeled as a rigid body, and the face sheet and foam core was modeled using 4-node shell (S4R) and 8-node linear brick (C3D8R) finite elements, respectively. The finite element mesh was condensed towards center of sandwich beam. The type of the contact between the face sheet and foam core was *TIE. The indenter has a constant vertical velocity of 1 m/s, and the lower and edge boundaries of the sandwich beam were fully clamped.

The mechanical properties of face sheet material were obtained from the stainless steel Cr18Ni8 with Young's modulus $E = 200$ GPa, Poisson's ratio $\nu = 0.3$, and the engineering stress-strain hardening data are cited from reference [9] and shown in Table 1. The flow stress $\sigma_0 = 602.5$ MPa was calculated from the average of yield stress and ultimate stress.

The plastic part of the mechanical behavior of the core was modeled using the *CRUSHABLE FOAM and the *CRUSHABLE FOAM HARDENING options in the ABAQUS package. The mechanical properties of foam for various relative densities are given as follows [9]

Table 1. Strain hardening data for stainless steel Cr18Ni8 [9].

Plastic strain (%)	Stress (MPa)	Plastic modulus (MPa)
0.0	507	1562.5
4.8	570	1041.6
9.8	620	729.2
14.8	655	416.7
19.8	675	208.3
24.8	685	104.2
29.8	698	20.83

$$E_f = E_s(\rho_f/\rho_s)^2 \quad (29)$$

and

$$\sigma_p = \sigma_{0,s}(\rho_f/\rho_s)^{3/2} \quad (30)$$

where E_f is the Young's modulus of foam, and ρ_f is its density. E_s , $\sigma_{0,s}$, and ρ_s are the Young's modulus, plastic flow stress, and mass density of solid cell wall of the foam material, respectively. The Young's modulus is obtained from reference [10], while the plateau stress of the foam is obtained from reference [11]. The flow stress and Young's modulus of the solid cell wall foam are $\sigma_{0,s} = 111.4$ MPa and $E_s = 94.1$ GPa, respectively [9]. Additionally, densification process was considered and described by initial densification strain $\varepsilon_D^{\text{initial}}$ and full densification one $\varepsilon_D^{\text{full}}$, defined by [10]

$$\varepsilon_D^{\text{initial}} = 1 - 1.4(\rho_f/\rho_s) \quad (31)$$

and

$$\varepsilon_D^{\text{full}} = 1 - \rho_f/\rho_s \quad (32)$$

respectively.

Compressive stress sharply rises from plateau stress to flow stress of the solid cell wall, according to strain from $\varepsilon_D^{\text{initial}}$ to $\varepsilon_D^{\text{full}}$, as depicted in Figure 2. In the finite element analysis, they are required to transform to logarithmic strain.

Results and discussion

Dimensionless form of theoretical predictions

We introduce a dimensionless parameter

$$\varphi = \frac{\sigma_p R}{\sigma_0 h} \quad (33)$$

which is related to the ability of the resistance of the sandwich structure to localized indentation deformation. This dimensionless parameter is usually small due to the low strength of core material. Some other dimensionless parameters are defined as

$$\bar{x} = \frac{x}{R}, \quad \bar{\xi} = \frac{\xi}{R}, \quad \bar{a} = \frac{a}{R}, \quad \bar{w} = \frac{w}{R}, \quad \bar{\delta} = \frac{\delta}{R}, \quad \bar{P} = \frac{P}{\sigma_0 b h} \quad (34)$$

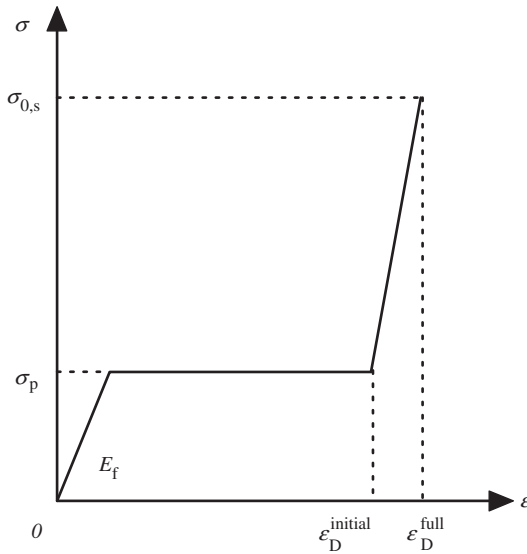


Figure 2. Uniaxial compressive characteristic of foam material.

For the loading of the flat indenter, the theoretical predictions have been presented in Equations (11), (12), (16), and (18), which can be rewritten in dimensionless form by

$$\bar{\xi} = 1 + (2\bar{\delta}/\varphi)^{1/2} \tag{35}$$

$$\bar{P} = 2\varphi + 2(2\varphi\bar{\delta})^{1/2} \tag{36}$$

$$\bar{w} = \bar{\delta} \left(\frac{\bar{\xi} - |\bar{x}|}{\bar{\xi} - 1} \right)^2, \quad 1 \leq |\bar{x}| \leq \bar{\xi} \tag{37}$$

and

$$\alpha = 1 + 3(\varphi/2\bar{\delta})^{1/2} \tag{38}$$

respectively.

For the loading of the cylindrical indenter, we use the same dimensionless parameters as defined above and then we have the following relations:

$$\bar{a} = \left(\frac{2\varphi\bar{\delta}}{1 + \varphi} \right)^{1/2} \tag{39}$$

$$\bar{\xi} = \left[\left(1 + \frac{1}{\varphi} \right) 2\bar{\delta} \right]^{1/2} \quad (40)$$

$$\bar{P} = 2[2\varphi(1 + \varphi)\bar{\delta}]^{1/2} \quad (41)$$

$$\bar{w} = \left(\bar{\delta} - \frac{\bar{a}^2}{2} \right) \left(\frac{\bar{\xi} - |\bar{x}|}{\bar{\xi} - \bar{a}} \right)^2, \quad \bar{a} \leq |\bar{x}| \leq \bar{\xi} \quad (42)$$

$$\alpha = 1 + 2\varphi \quad (43)$$

Indentation force

In the theoretical modeling, the influences of the length of the sandwich beam and thickness of the foam core are not considered. To keep consistency, the length of the sandwich beam and thickness of the foam core are set to be 200 mm and 25 mm in the numerical simulation, respectively. Values of other parameters selected are listed in Table 2.

The indentation force of flat indenter, as predicted in Equation (12), indicates that it has an initial value at zero indentation displacement and varies linearly with the square root of indentation displacement. The initial value is proportional to the width of the indenter and remains constant during denting. It is due to the compressive deformation of foam core just under the indenter. For a small indentation displacement, there is a slight difference from the simulated result involved in the elastic response. However, the simulated force rapidly rises and reaches the initial value in a very short displacement, as shown in Figure 3.

The indentation force of cylindrical indenter from the analytical model, as predicted in Equation (25), also varies linearly with the square root of indentation displacement but does not have an initial value due to a zero contact region at the initial indentation displacement. A comparison between the theoretical force and the simulated force is shown in Figure 4.

For both types of indenters, slight differences between the theoretical forces and the simulated forces appear at moderate indentation displacements, especially for

Table 2. Parameter values selected for the comparison.

ρ_f/ρ_s	h (mm)	R (mm)	σ_p (MPa)	φ
0.05	2	5	1.245	0.0052
0.1	2	5	3.523	0.0146
0.1	2	10	3.523	0.0292
0.1	1	10	3.523	0.0584

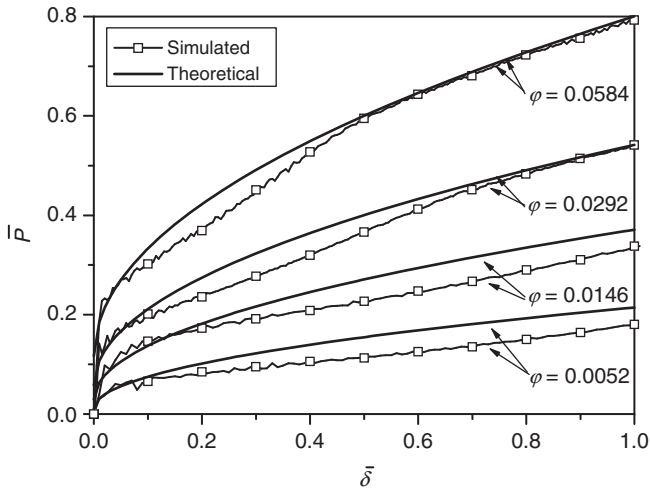


Figure 3. Indenter force–displacement curves under a flat indenter.

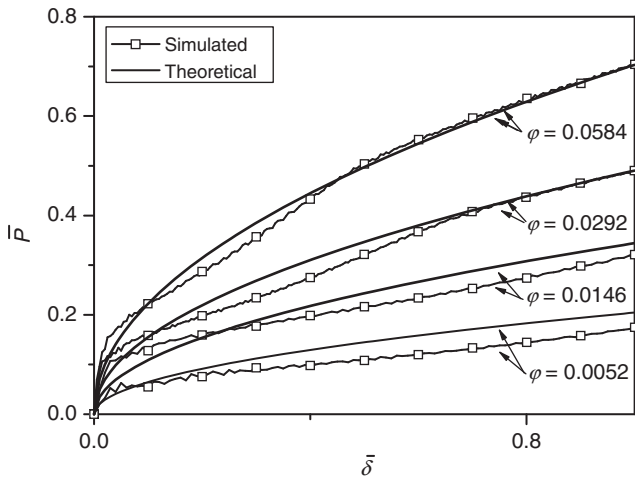


Figure 4. Indenter force–displacement curves under a cylindrical indenter.

the case of $\varphi = 0.0052$. For a high value of φ , the theoretical predictions are better in agreement with the simulated results.

Profiles of the deformation zone

The assumption of the velocity field of the dented zone is the basis of theoretical analysis, which directly determines its operability and validity. Its validity could be verified by comparing the profiles of the deformation zone from theoretical model with those from numerical simulation. The theoretical and simulated results for the

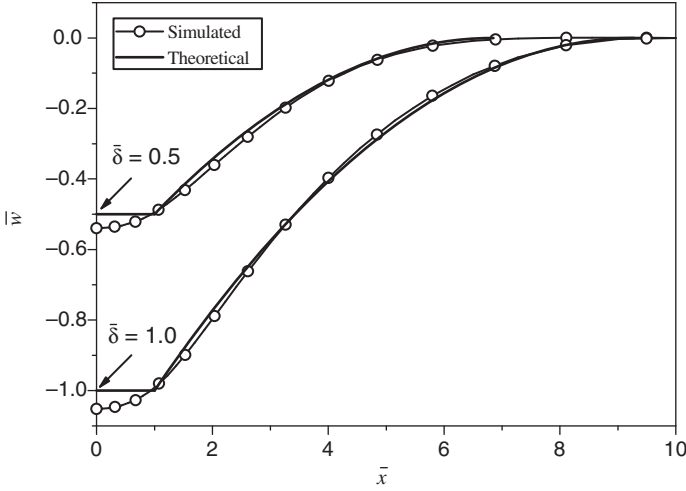


Figure 5. Distribution of deformation for $\varphi = 0.0292$ under a flat indenter.

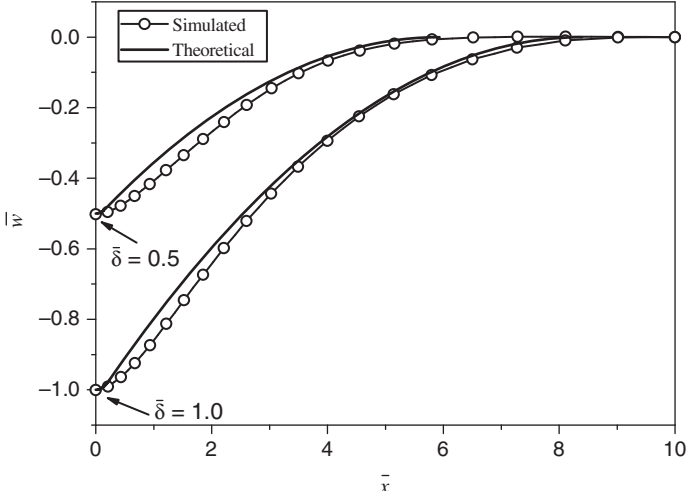


Figure 6. Distribution of deformation for $\varphi = 0.0292$ under a cylindrical indenter.

cases of flat indenter and cylindrical indenter with $\varphi = 0.0292$ are shown in Figures 5 and 6, respectively. The comparisons have shown that the theoretical predictions agree well with the simulated results except for some details. For the loading of the flat indenter, simulated results indicate that the central part of the face sheet under flat indenter separates from the indenter in the denting process, which was not considered in the analytical model. For the loading of the cylindrical indenter, a little discrepancy can be found in the areas closed to the contact region. Highly precise velocity field may help to improve the theoretical results.

Conclusions

Concisely explicit solutions for the localized indentation of sandwich beam with metallic foam core have been derived in this article. Two types of indenters, i.e., the flat and cylindrical indenters, have been considered. An approximation of linear velocity field was employed and the principle of virtual velocities was used to determine the indentation force and the distribution of displacement field of the deformed region. In the analytical models, the principle of minimum work was applied to determine range of deformation zones and contact region. The dimensionless indentation forces, dominated by one dimensionless characteristic parameter φ , vary linearly with square root of indenter displacement. The analytical formulations indicate that the surface deformation profiles are proportional to the square of the distance from contact center along the beam direction and size of indented dents decreases with increasing the characteristic parameters. These theoretical predictions agree well with the simulated results.

Funding

This work was supported by the National Natural Science Foundation of China (Projects Nos. 90916026, 10532020, and 10672156).

References

1. Gdoutos EE, Daniel IM and Wang KA. Indentation failure in composite sandwich structures. *Exper Mech* 2002; 42(4): 426–431.
2. Soden PD. Indentation of composite sandwich beams. *J Strain Anal Eng Des* 1996; 31(5): 353–360.
3. Shuaeib FM and Soden PD. Indentation failure of composite sandwich beams. *Compos Sci Technol* 1997; 57(9-10): 1249–1259.
4. Zenkert D, Shipsha A and Persson K. Static indentation and unloading response of sandwich beams. *Compos Part B Eng* 2004; 35(6-8): 511–522.
5. Koissin V, Shipsha A and Rizov V. The inelastic quasi-static response of sandwich structures to local loading. *Compos Struct* 2004; 64(2): 129–138.
6. Koissin V, Skvortsov V, Krahmalev S and Shilpsha A. The elastic response of sandwich structures to local loading. *Compos Struct* 2004; 63(3-4): 375–385.
7. Koissin V and Shipsha A. Residual dent in locally loaded foam core sandwich structures - analysis and use for NDI. *Compos Sci Technol* 2008; 68(1): 57–74.
8. Minakuchi S, Okabe Y and Takeda N. “Segment-wise Model” for theoretical simulation of barely visible indentation damage in composite sandwich beams: part I – formulation. *Compos Part A Appl Sci Manuf* 2008; 39(1): 133–144.
9. Santosa S, Banhart J and Wierzbicki T. Experimental and numerical analyses of bending of foam-filled sections. *Acta Mech* 2001; 148(1): 199–213.
10. Gibson LJ and Ashby MF. *Cellular solids: structure and properties*. Cambridge University Press.
11. Santosa S and Wierzbicki T. On the modeling of crush behavior of a closed-cell aluminum foam structure. *J Mech PhysSol* 1998; 46(4): 645–669.